



## SINGLE STEP SYNTHESIS OF H-MWCNTS AND ITS APPLICATION AS VISIBLE LIGHT DRIVEN PHOTOCATALYST IN DYE DEGRADATION STUDIES

A.SARAVANAN<sup>A</sup>, A. ABILARASU<sup>B</sup> AND T. SOMANATHAN<sup>A,\*</sup>

<sup>a</sup>*Department of Nanoscience, School of Basic Sciences*

<sup>b</sup>*Department of Chemistry, School of Basic Sciences Vels University, Pallavaram, Chennai-600 117, India*

### ABSTRACT

In this work, we have synthesized carbon nanotubes CNTs in a single step and tested for photocatalytic activity under visible light. The synthesized CNTs were characterized using XRD, SEM, HRTEM and Raman spectroscopy. The surface characterization of the CNTs reveals that the morphology seems to be helical multi walled carbon nanotubes (h-MWCNTs). The dependency of photodegradation to variables such as contact time, pH, catalyst weight, H<sub>2</sub>O<sub>2</sub> concentration and dye concentration were investigated and optimized. The results implies that the CNTs play a vital role in degradation studies at pH 3 with very trace amount of CNTs as a photocatalyst. This suggests that the ability of CNTs will able to store and shuttle the electrons available in the visible region for dye degradation which can possibly used in environmental remediation.

**KEY WORDS:** h-MWCNTs, in-situ, photocatalyst, pH study, Visible light driven catalyst



**T. SOMANATHAN**

Department of Nanoscience, School of Basic Sciences

\*Corresponding author

## 1. INTRODUCTION

Huge amount of waste generated from industry have become a major concern in the recent days and tremendous work is in progress to eradicate these issues on pollutant. The conventional treatment methods like secondary biodegradation or advanced treatment technologies such as activated carbon and reverse osmosis can produce high quality water. Even though they are only concentrating in transfer of pollutants from one phase to another, which requires further processing to render contaminate to be inert<sup>1</sup>. Recently, advanced oxidation processes (AOPs) are powerful and attractive techniques in treatment of highly organic loading and non-biodegradable wastewater<sup>2,3</sup>. Advanced oxidation processes helps in almost complete oxidation of organic pollutants through reactions with hydroxyl radicals that are generated from ozone or H<sub>2</sub>O<sub>2</sub><sup>4,5</sup>. However, these techniques have certain limitation in application<sup>6</sup>, such as electron hole recombination, very less % of UV composition in sun light at shorter wavelength (400 nm). Tuning of visible light driven (VLD) catalyst overcomes this defect to improve some of the main aspects like active sites, electron-hole recombination and effective usage of visible light with band-gap modification. Particularly, great efforts have been devoted to the preparation of semiconducting photocatalyst composites to improve the utilization of visible light<sup>7-9</sup>. While considering photo catalyst, carbon nanotubes (CNTs) composites have attracted researchers because CNTs are 1D carbon-based ideal molecule with the nanocylinders, which can conduct electricity at room temperature with essentially no resistance. This phenomenon is known as ballistic transport, by which the electrons are considered to move freely through the structure, without any scattering from atoms or defects. In this work, we have synthesized CNTs from combustion catalyst and studied its photocatalytic activity after purification against congo red dye. The efficiency of the photocatalyst is increased due to the reduction of electron/hole pair

recombination and also the effective usage of visible light by CNTs.

## 2. EXPERIMENTAL

### 2.1 Catalyst preparation

According to our previous report<sup>10,11</sup> the Fe<sub>0.25</sub>Ni<sub>0.09</sub>Mg<sub>0.66</sub>O catalyst was prepared from the aqueous solutions of corresponding metal nitrates with citric acid as combustion agent using CVD technique<sup>12</sup>. Further catalyst was reduced using Hydrogen gas flow (150 SCCM) from 550°C to 700°C. Then the carbon source acetylene was purged (100 SCCM) into the CVD system for 10 min to CNTs synthesis. After completion of the reaction, the N<sub>2</sub> gas flow was purged to cool the CVD system under inert atmosphere. The pristine CNTs were purified by stirring with Conc. HCl (35%) for 2hr and then washed with distilled water for several times until it becomes neutral<sup>13</sup>.

### 2.2 Photocatalytic activity of CNTs

The dye degradation studies were done using the purified CNTs. The synthesized carbon products were suspended in 50ml of the aqueous congo red dye (CRD) solution. Then the dye solution was placed in dark for half an hour to establish adsorption equilibrium. To this resultant solution H<sub>2</sub>O<sub>2</sub> was added as oxidising agent and degradation studies were carried out under direct sunlight. At regular intervals of time the solution was collected and centrifuged (to remove the catalyst). The dye degradation was monitored using UV spectrometer.

### 2.3 Characterization of catalyst

The purified CNTs morphology was characterized using scanning electron microscopy (SEM) image JEOL, JSM6390. High resolution transmission electron microscope (HRTEM) was done with Technai T30 300 Kev Brand FEI. X-ray diffraction (XRD) measurement was carried out for phase identification using CuK $\alpha$ ,  $\lambda=0.1541$  nm on G.E Inspection Technologies, model no XRD 3003 TT. Raman spectroscopy was done through

Bruker: RFS27 FT Raman using Nd:YAG laser at a 1064nm wavelength. The catalytic activity was measured by Shimadzu UV-3600 Model UV-Visible Spectrophotometer (Japan) scanning from 200 nm to 800nm.

### 3. RESULTS AND DISCUSSION

#### 3.1 Characterisation of purified CNTs

##### 3.1.1 XRD pattern of purified CNTs

The XRD analysis was employed to study the diffraction patterns of purified CNTs. As shown in Fig. 1 diffraction pattern peaks at  $2\theta = 25.8$  and  $43.04$  are corresponding to the (002) and (100) reflections of typical graphite (JCPDS 41-1487)<sup>14-16</sup>. The strong peak at (002) planes of the purified CNTs shows the good degree of crystallinity with absence of amorphous carbon. Also the XRD pattern of purified CNTs clearly shows the absence of metal impurities.

##### 3.1.2 SEM images of MWCNTs

The morphology of purified CNTs prepared using  $\text{Fe}_{0.25}\text{Ni}_{0.09}\text{Mg}_{0.66}\text{O}$  metal catalyst was shown in Fig. 2. Fig. 2a shows FESEM image of the purified CNTs with a bundle of CNTs which magnified under low magnification. Fig. 2b clearly indicates the helical structure of the purified CNTs. From the SEM image we clearly infer that the purified CNTs are almost helical in nature. Fig. 2c shows the EDX pattern for purified CNTs and the results were tabulated in Table 1.

##### 3.1.3 HRTEM of helical MWCNTs

The HRTEM images of the purified CNTs are shown in Fig. 3. In which Fig. 3a shows the helical nature of the CNTs with almost identical diameter, length and pitch. Fig. 3b infers the parallel wall structure of the h-MWCNTs with some nanoparticles buried inside it, where the size of nanoparticles is found to be in the range of 1-2nm a much smaller size than the internal diameter 4-5nm of CNTs. A similar observation is also reported in our earlier work<sup>10,17</sup>. The nano particle present in trace amount inside h-

MWCNTs may play a crucial role for the photocatalytic degradation of dye.

##### 3.1.4 Raman Spectra of purified CNTs

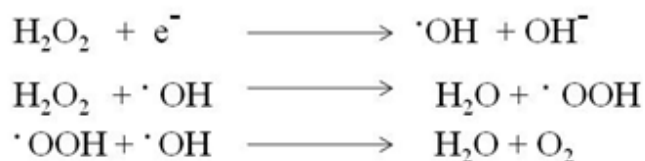
The nature of CNTs is best explained by Raman spectroscopy with the graphitic band (G band) and disordered band (D band). Fig. 4 shows the Raman spectra of the purified CNTs in which two prominent peaks located at  $1290\text{cm}^{-1}$  and  $1595\text{cm}^{-1}$  are corresponds to D band and G band. No peaks were observed in the lower region (under  $250\text{cm}^{-1}$ ) which clearly indicates the absence of SWCNTs and also confirms that the obtained CNTs are MWCNTs<sup>18,19</sup>. The  $I_G/I_D$  ratio of the purified CNTs is found to be 0.97 this is due to the strong D band which has resulted from lattice distortion of graphite layers in helical CNTs.

#### 3.2 Catalytic performance of CNTs on Congo Red dye (CRD) degradation

Photocatalytic study of the CNTs was carried out against CRD under direct sun light. The Fig.5 shows the comparative study of the adsorption and photodegradation of CRD using CNTs. The degradation result implies that the purified CNTs can act as a very good photocatalyst than adsorbent. The different reaction parameters such as catalyst concentration, pH,  $\text{H}_2\text{O}_2$ , and initial concentration of dye was investigated have been explained following sections.

##### 3.2.1 Effect of $\text{H}_2\text{O}_2$ dosage

In this study, the dosage of  $\text{H}_2\text{O}_2$  was varied from 0.1mL to 0.5mL, by keeping constant the catalyst concentration (30mg/L) and the initial pH 3. Fig. 6 shows the photocatalytic degradation efficiency increases with increase in  $\text{H}_2\text{O}_2$  dose from 0.1mL to 0.3mL. Further increase in  $\text{H}_2\text{O}_2$  dosage, the degradation efficiency decreases due to auto decomposition of  $\text{H}_2\text{O}_2$  and the excess formation of peroxy radical ( $\cdot\text{OOH}$ ) prior to form  $\cdot\text{OH}$  radicals which reduces the rate of degradation of dyes<sup>20,21</sup>.



### 3.2.2 Effect of CNTs dosage

The amount of CNTs has an important role on degradation of CRD. The serious of reaction was carried out at different dosage of CNTs from 0.02g/L to 0.08g/L. which is clearly indicated in Fig. 7. CNT dosage on increasing (0.020g to 0.030g) the photocatalytic degradation will increase due to the availability of active sites on the CNTs. Further increase in CNTs dosage (0.030g) degradation efficiency decreases this is due to scattering effect of the CNTs which reduces the penetration of light into the solution. Therefore, we concluded that excess amount of CNTs supply is unfavorable for the increase of photocatalytic degradation as a result of a lower light penetration<sup>22</sup>.

### 3.2.3 Effect of initial dye concentration

Fig. 8 shows the photocatalytic dye degradation for the different initial dye concentration. The dye concentration was varied from 0.020g/L – 0.05g/L while the other variables were kept constant. We found that the maximum degradation was obtained at 0.02g/L dye concentration. When initial dye concentration increases, the degradation tends to decrease due to the dye molecules to react with hydroxyl radical. Thus the dye degradation rate decreases.

### 3.2.4 Effect of pH

The pH value has a played a vital role on the degradation of the pollutants. It is known that the solution pH can affect the surface charge of the adsorbent, the degree of ionization of the different pollutants, the dissociation of functional groups on the active sites of the adsorbent as well as the structure of the dye molecule<sup>23</sup>. The effect of pH on the Congo Red dye degradation of the CNTs was conducted by varying pH 1-10 with 0.020g/L fixed initial dye concentrations and CNT dosage 0.030g for 90 min. Fig. 9 shows the degradation of dye by varying the pH. The degradation efficiency of dye increases with increasing solution pH from 1 to 3 and decreases slightly when solution pH is above 3. This suggests that the dye degradation is maximum at pH 3. It is well known that the surface of CNTs contains some oxygen groups such as carboxylic groups (-COOH) and hydroxyl groups (-OH) after acid treatment<sup>24</sup>. At lower pH 1, catalyst dissolution occurs there by it reduces the catalytic activity and at that the same time above pH 5 the degradation is found to be good but lesser than the acidic pH 3. Similar results were reported by other investigators<sup>25-28</sup>. At pH 3, the maximum reaction time was limited to 90 min this is due to the reason that the dye degradation attained equilibrium and further increasing the degradation time there is no change in the degradation.

**Table 1**  
**Elemental content from EDAX analysis**

<i>Element</i>	<i>Wt %</i>	<i>At %</i>
<b>CK</b>	<b>85.61</b>	<b>90.08</b>
<b>OK</b>	<b>11.07</b>	<b>08.74</b>
<b>MgK</b>	<b>01.47</b>	<b>00.77</b>
<b>FeK</b>	<b>01.00</b>	<b>00.23</b>
<b>NiK</b>	<b>00.84</b>	<b>00.18</b>

**Figure 1**  
**XRD pattern of Purified CNTs**

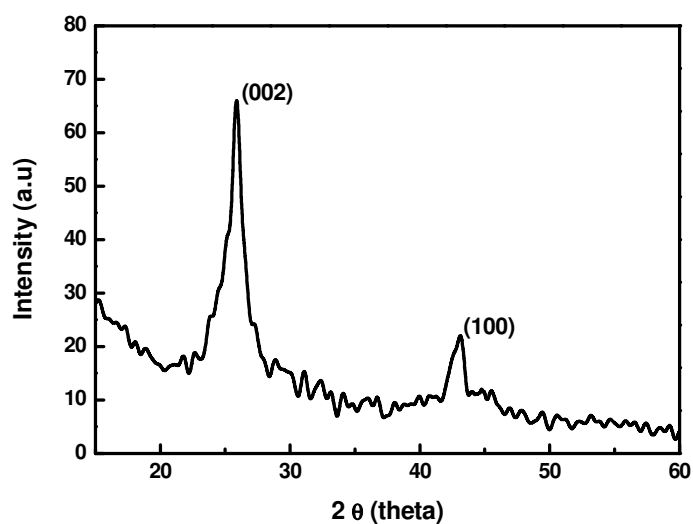


**Figure 2**  
**FESEM & EDAX images of purified CNTs**

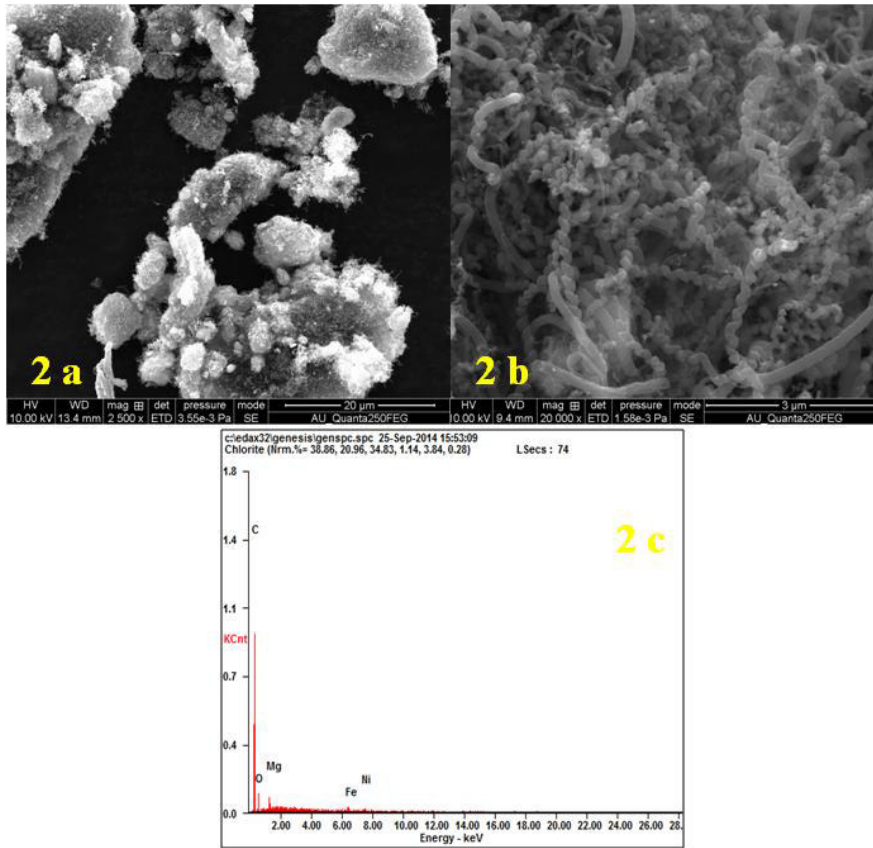


**Figure 3**  
**HRTEM image of h-MWCNTs**

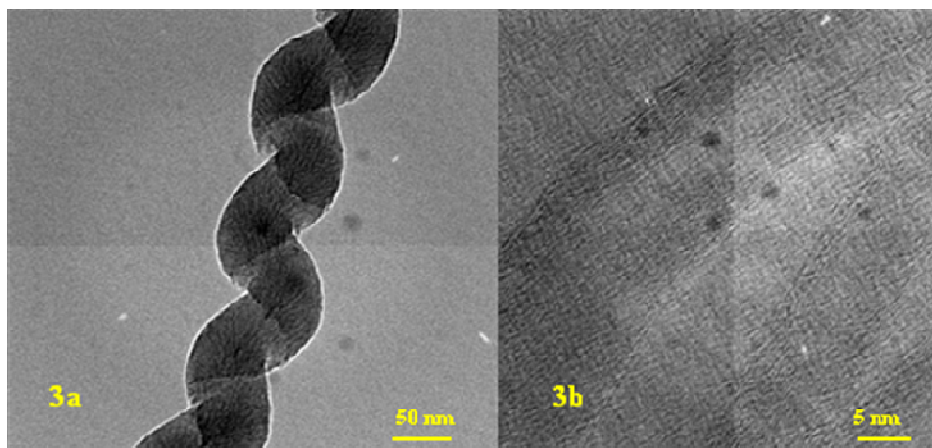


**Figure 4**  
*Raman spectra of purified h-MWCNTs*

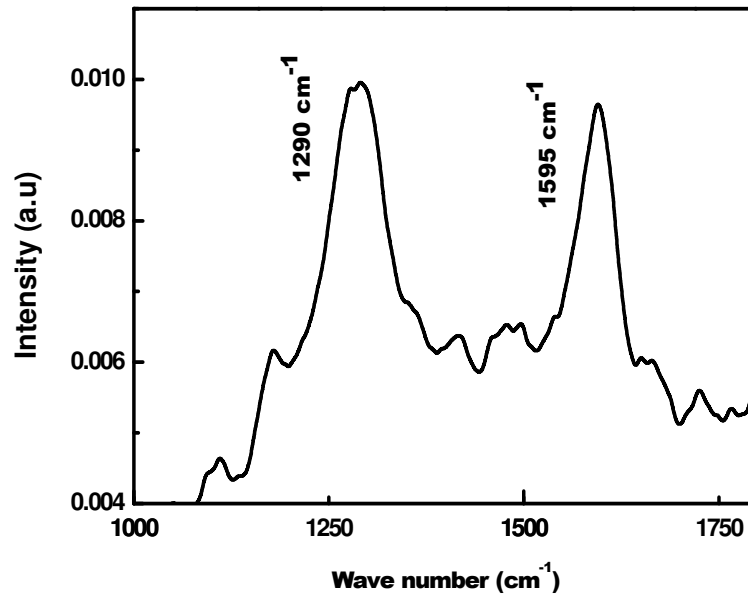


**Figure 5**  
*Photocatalytic effect of purified CNTs*

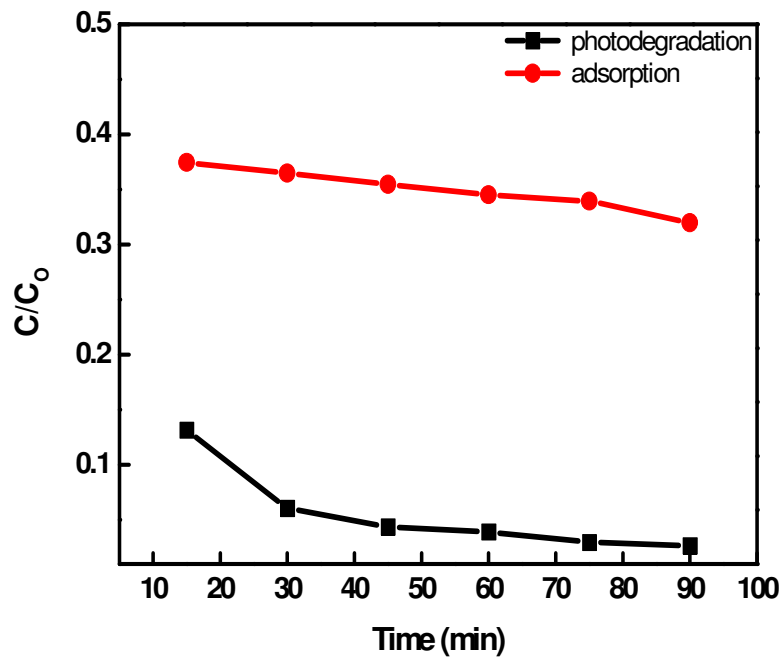


**Figure 6**  
*Role of H<sub>2</sub>O<sub>2</sub> concentration on degradation studies*

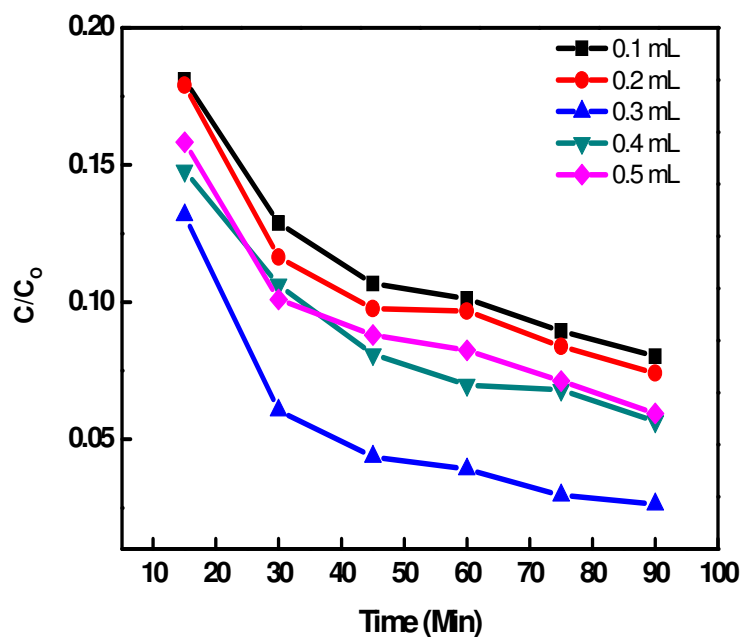


**Figure 7**  
*Effect of catalyst weight*

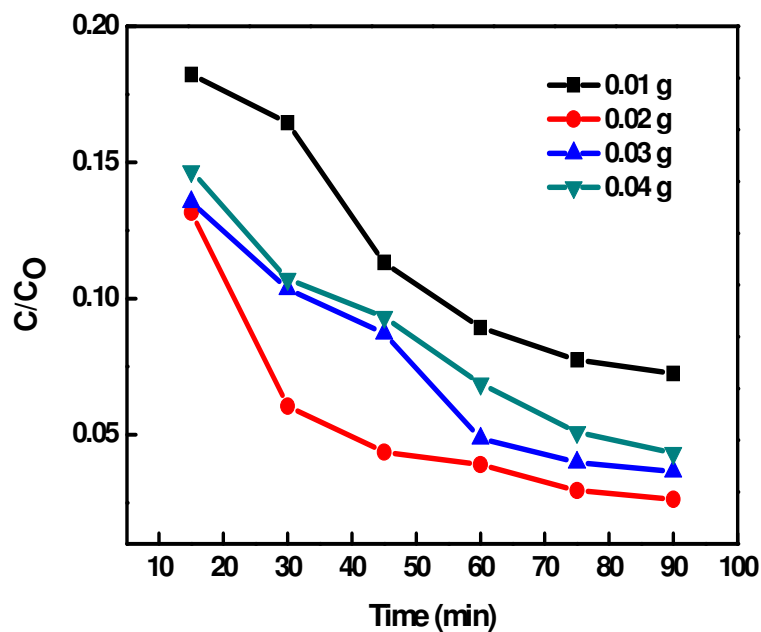




**Figure 8**  
*Influence of dye concentration on degradation studies*

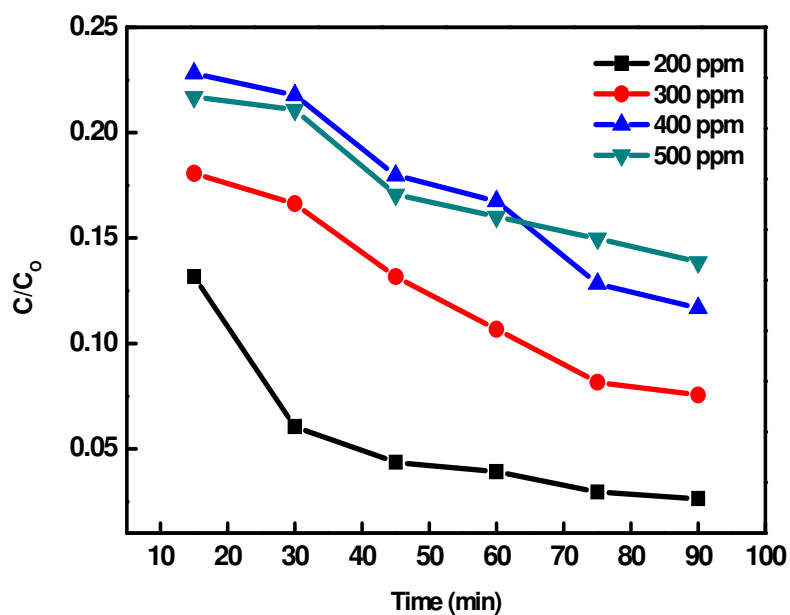
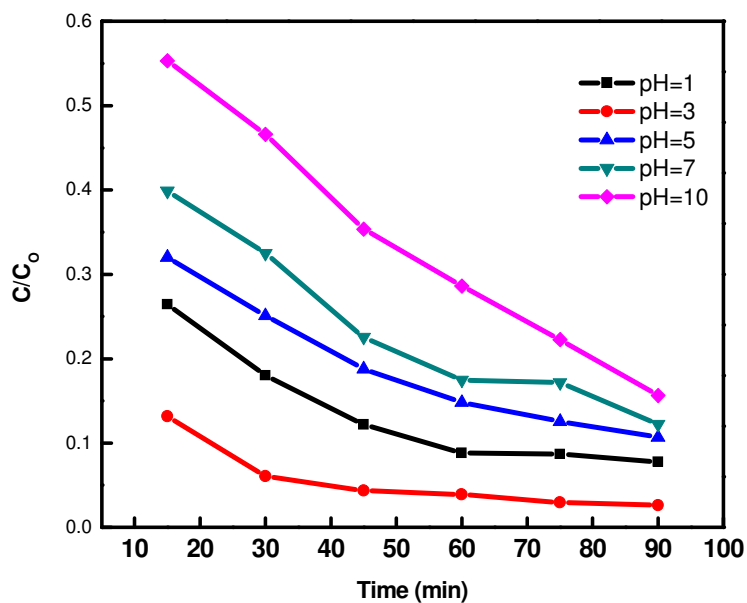


**Figure 9**  
*Influence of pH on dye degradation*



## 4. CONCLUSION

In this present work we have synthesized and characterized the purified CNTs. XRD indicates that the CNTs have a very good crystallinity in nature which also confirmed by FESEM and HRTEM analysis. HRTEM indicates that the CNTs are helical in nature and multi layer of the tubes which is clearly evident by Raman spectroscopy. The purified CNTs were used as photo catalyst for dye degradation studies. The effect of initial dye concentration, H<sub>2</sub>O<sub>2</sub>, CNT dosage and pH on the photocatalytic dye degradation were evaluated. The result shows that the purified CNTs act as an efficient photocatalyst in a short span of time with a small amount of catalyst at pH 3. Consequently, it can be concluded that

the synthesized CNTs could be used as potential photocatalyst to degrade organic pollutant in aqueous media.

## ACKNOWLEDGEMENT

The Author A. Saravanan would like to thank the Vels University, Pallavaram, Chennai for providing the University Fellowship and also one of the authors, T. Somanathan would like to thank the Department of Science and Technology (DST) for the award of Fast Track Young Scientist Award by providing financial support (SR/FT/CS-111/2011).

## REFERENCES

1. Devagi K., Glass B.D., Oelgemöller M. Titanium dioxide photocatalysis for pharmaceutical wastewater treatment, *Environ. Chem. Lett.*, 12(1): 27–47, (2014)
2. Wang Y., Zhao H., Gao J., Zhao J., Zhang Y., Zhang. Rapid mineralization of azo-dye wastewater by microwave synergistic electro-Fenton oxidation process, *J. Phys. Chem. C*, 116(13): 7457–7463, (2012)
3. Tušar N.N., Mauček D., Rangus M., Arčon I., Mazaj M., Cotman M., Pintar A., Kaučič V. Manganese functionalized silicate nanoparticles as a Fenton-type catalyst for water purification by advanced oxidation processes (AOP), *Adv. Funct. Mater.*, 22(4): 820–826, (2012)
4. Zhang T., Zhu H., Croué J.P. Production of sulfate radical from peroxymonosulfate induced by a magnetically separable CuFe<sub>2</sub>O<sub>4</sub> spinel in water: efficiency, stability, and mechanism, *Environ. Sci. Technol*, 47(6): 2784–2791, (2013)
5. Subbaramaiah V., Srivastava V.C., Mall I.D. Optimization of reaction parameters and kinetic modeling of catalytic wet peroxidation of picoline by Cu/SBA-15, *Ind. Eng. Chem. Res.*, 52(26): 9021–9029, (2013)
6. Yuan S., Fan Y., Zhang Y., Tong M., Liao P. Pd-catalytic in situ generation of H<sub>2</sub>O<sub>2</sub> from H<sub>2</sub> and O<sub>2</sub> produced by water electrolysis for the efficient electro-Fenton degradation of Rhodamine B, *Environ. Sci. Technol.* 45(19): 8514–8520, (2011)
7. Saleh T.A., Gondal M.A., Drmosh Q.A., Yamani Z.H., AL-yamani. A Enhancement in photocatalytic activity for acetaldehyde removal by embedding ZnO nano particles on multiwall carbon nano. *Chem. Eng. J.* 166(1): 407–412, (2011).
8. Peng T.Y., Zeng P., Ke D.N., Liu X.J., Zhang X.H. Hydrothermal preparation of multiwalled carbon nanotubes (MWCNTs)/CdS nanocomposite and its efficient photocatalytic hydrogen production under visible light irradiation. *Energy Fuels*, 25(5): 2203–2210, (2011)
9. Xu Y.G., Xu H., Yan J., Li H.M., Huang L.Y., Zhang Q., Huang C.J., Wan H.L. A novel visible-light-response plasmonic photocatalyst CNT/Ag/AgBr and its photocatalytic properties. *Phys. Chem. Chem. Phys.* 15(16): 5821–5830, (2013)

10. Saravanan A., Karthika P., Gokulakrishnan N., Kalaivani R.A., Somanathan T. Efficiency of transition metals in combustion catalyst for high yield helical multiwalled carbon nanotubes, *Adv. Sci. Eng. Med.* 6(7): 809-813, (2014)
11. Abilarasu, Saravanan A., Somanathan T. Synthesis of cobalt doped manganese ferrite and it used as a visible active fenton catalyst for dye degradation, *Journal of Chemical and Pharmaceutical Sciences*, (4):111-112, (2014)
12. Mohana Krishna V., Somanathan T. Electrocatalytic activity of bamboo-like multi walled carbon nanotubes for the determination of ascorbic acid, *Int. J. Pharm. Bio. Sci.*, 6(3): 239 – 245, (2015)
13. Somanathan T., Pandurangan A. Helical multiwalled carbon nanotubes (*h*-MWCNTs) synthesized by catalytic chemical vapor deposition, *New Carbon Materials*, 25(3):175–180, (2010)
14. Li W.B., Zhai D., Pa L., Pu L., Xu J., Shia J. Synthesis of Multishell Carbon Nanotube Composites via Template Method, *Chin. J. Chem. Phys.*, 24(2): 206-210, (2011)
15. Atchudan R., Pandurangan A., Somanathan T. Bimetallic mesoporous materials for high yield synthesis of carbon nanotubes by chemical vapour deposition techniques, *J. Mol. Catal. A: Chem.*, 309(1): 146–152, (2009)
16. Shitole K.D., Nainani R.K., Pragati T. Preparation, characterisation and photocatalytic applications of TiO<sub>2</sub>-MWCNTs Composite, *Defence Science Journal*, 63(4): 435-441, (2013)
17. Saravanan A., Somanathan T., Mohana Krishna V. In situ synthesis of carbon nanotubes through combustion Technique, *Int.J. ChemTech Res.*, 7(3):1639-1643, (2015)
18. Somanathan T., Pandurangan A. Towards the low temperature growth of uniform diameter multi walled carbon nanotubes by catalytic chemical vapour deposition technique, *Nano-Micro Lett.*, 2(3): 204-212, (2010)
19. Somanathan T., Balaji M., Vidhya E. Synthesis of highly graphitised few walled carbon nanotubes by chemical vapour deposition technique, *International journal of frontiers in science and technology*, 1(1): 42-46, (2013)
20. Muthukumari B., Selvam K., Muthuvel I., Swaminathan M. Photoassisted hetero-Fenton mineralisation of azo dyes by Fe(II)-Al<sub>2</sub>O<sub>3</sub> catalyst, *Chemical Engineering Journal* 153: 9–15 (2009)
21. Nguyen T.D., Phan N.H., Do M.H., Ngo K.T., Magnetic Fe<sub>2</sub>MO<sub>4</sub> (M:Fe, Mn) activated carbons: Fabrication, characterization and heterogeneous Fenton oxidation of methyl orange, *Journal of Hazardous Materials*, 185(2-3): 653–661, (2011)
22. Li D., Wang S., Wang J., Xiaodan Z., Liu S. Synthesis of CdTe/TiO<sub>2</sub> nanoparticles and their photocatalytic activity', *Materials Research Bulletin*, 48(10): 4283-4286, (2013)
23. Ai L., Zhang C., Liao F., Wang Y., Li M., Meng L., Jiang J. Removal of methylene blue from aqueous solution with magnetite loaded multi-wall carbon nanotube: Kinetic, isotherm and mechanism analysis, *Journal of Hazardous Materials*, 198: 282– 290, (2011)
24. Liu Z., Rinzler A.G., Dai H., Hafner J.H., Bradley R.K., Boul P.J., Lu A., Iverson T., Shelimov K., Huffman C.B., Macias F.R, Shon Y.S., Lee T.R., Colbert D.T., Smalley R E, Fullerene Pipes, *Science*, 280(5367): 1253-1256, (1998)
25. Shirmard M., Mesdaghinia A., Mahvi A. H., Nasserli S., Nabizadeh R. Kinetics and Equilibrium Studies on Adsorption of Acid Red 18 (Azo-Dye) Using Multiwall Carbon Nanotubes (mwcnts) from Aqueous Solution, *E-Journal of Chemistry*, 9(4): 2371-2383, (2012)
26. Zhu H.Y., Yao J., Jiang R., Fu Y.Q., Wu Y.H., Zeng G.M., Enhanced decolorization of azo dye solution by cadmium sulfide/multi-walled carbon nanotubes/polymer composite in combination with hydrogen peroxide under

- simulated solar light irradiation, *Ceramics International*, 40(2): 3769–3777, (2014)
27. Saquib M., Abu Tariq M., Haque M.M., Muneer M. Photocatalytic degradation of disperse blue 1 using UV/TiO<sub>2</sub>/H<sub>2</sub>O<sub>2</sub> process, *Journal of Environmental Management*, 88(2): 300–306, (2008)
28. Li G., Zhao X.S., Ray M.B. Advanced oxidation of orange II using TiO<sub>2</sub> supported on porous adsorbents: the role of pH, H<sub>2</sub>O<sub>2</sub> and O<sub>3</sub>, *Separation and Purification Technology* 55(1): 91–97, (2007)